Science Advances
AAAS

advances.sciencemag.org/cgi/content/full/5/11/eaax0629/DC1

Supplementary Materials for

Fibrinogen-like protein 2 controls sepsis catabasis by interacting with resolvin Dp5

Yu Zhou, Juan Lei, Qichao Xie, Lei Wu, Shengwei Jin, Bo Guo, Xiang Wang, Guifang Yan, Qi Zhang, Huakan Zhao, Jiangang Zhang, Xiao Zhang, Jingchun Wang, Jiaqi Gu, Xiaoli Liu, Duyun Ye, Hongming Miao*, Charles N. Serhan*, Yongsheng Li*

*Corresponding author. Email: hongmingmiao@sina.com (H.M.); cserhan@bwh.harvard.edu (C.N.S.); yli@tmmu.edu.cn (Y.L.)

Published 13 November 2019, *Sci. Adv.* **5**, eaax0629 (2019)
DOI: 10.1126/sciadv.aax0629

This PDF file includes:

Table S1. Characteristics of patients. WBC, white blood cells; CRP, C-reactive protein; PCT, procalcitonin; PLT, platelet; PT, Prothrombin time; INR, International Normalized Ratio; FIB, fibrinogen; TT, thrombin time; APTT, activated partial thromboplastin time.

Control													
Samples	Sex	Age	Etiology	APACHE II scores	CRP	PCT	Creatine	Lactate	PT	INR	FIB	TT	DD	APTT
n1	Male	48	Healthy	7	5.3	3.41	42	1.1	10.3	1.1	2.1	13.0	2.5	28.35
n2	Male	30	Healthy	5	2.2	5.29	57	0.5	10.5	1.5	3.0	13.5	3.8	26.53
n3	Male	59	Healthy	8	3.4	11.03	59	0.9	11.6	1.3	3.4	16.8	4.7	28.79
n4	Male	33	Healthy	5	3.8	3.55	74	0.8	12.3	1.7	2.6	16.1	3.4	30.02
n5	Male	49	Healthy	7	7.6	6.46	59	1.3	12.8	1.4	1.9	16.7	3.3	26.57
n6	Male	52	Healthy	7	5.5	2.07	68	2.2	13.3	1.4	2.2	15.9	4.5	27.44
n7	Female	54	Healthy	7	8.1	1.08	73	1.4	13.2	1.3	3.1	16.4	6.3	25.76
n8	Female	47	Healthy	6	7.0	1.55	82	1.2	10.9	1.5	3.5	17.5	4.6	29.45
n9	Female	43	Healthy	5	3.5	3.82	79	0.6	11.5	1.9	2.7	15.6	4.1	35.84
n10	Female	56	Healthy	8	6.4	3.17	68	0.8	11.9	1.4	2.6	16.8	3.2	32.71
n11	Female	51	Healthy	7	2.3	2.86	82	0.7	12.4	1.6	3.5	16.7	5.5	33.15
n12	Female	42	Healthy	5	7.5	2.22	77	1.3	13.1	1.0	2.4	13.9	6.1	30.94
Sepsis Survivors														
Samples	Sex	Age	Etiology	APACHE II scores	CRP	PCT	Creatine	Lactate	PT	INR	FIB	TT	DD	APTT
n1	Male	29	Klebsiella pneumoniae	16	12.5	3.30	15	2.3	12.5	1.5	1.5	16.9	0.8	29.63
n2	Male	33	Staphylococcus aureus	18	43.8	41.40	28	6.5	13.6	1.2	2.7	19.5	1.9	46.52
n3	Male	37	Streptococcus pneumoniae	19	49.3	12.50	19	4.8	19.9	1.4	4.4	19.8	9.7	36.72
n4	Male	39	Staphylococcus aureus	21	121.2	18.50	33	9.1	15.3	1.6	3.3	17.5	6.5	38.45
n5	Male	52	Enterobacter aerogenes	24	97.5	16.90	59	5.3	16.8	1.7	5.8	17.3	4.3	33.91
n6	Male	62	Candida albicans	23	185.4	22.70	54	3.7	17.9	1.3	6.7	19.2	4.2	42.83
n7	Female	60	Escherichia coli	24	135.3	32.60	38	3.9	14.5	1.0	7.2	19.1	3.5	40.61
n8	Female	42	Haemophilus	19	121.7	49.80	43	5.8	16.3	1.4	3.7	18.4	2.9	41.72
n9	Female	43	Candida albicans	18	163.5	50.30	42	4.3	18.1	1.5	8.3	18.6	6.4	30.91
n10	Female	51	Streptococcus pneumoniae	21	124.7	21.80	31	5.5	16.6	1.6	6.5	17.8	8.1	42.40
n11	Female	58	Escherichia coli	20	115.9	15.67	94	6.1	14.8	1.8	7.5	20.3	7.8	43.65
n12	Female	47	Candida albicans	22	87.8	30.41	72	7.4	16.4	1.3	7.8	19.8	6.9	49.88
Sepsis non-survivors														
Samples	Sex	Age	Etiology	APACHE II scores	CRP	PCT	Creatine	Lactate	PT	INR	FIB	TT	DD	APTT
n1	Male	33	Pseudomonas aeruginosa	23	43.5	0.90	63	6.7	13.1	1.3	2.2	17.4	0.9	38.81
n2	Male	59	Pseudomonas aeruginosa	29	148.0	1.50	78	2.5	15.8	1.7	3.5	18.3	1.5	39.50
n3	Male	46	Acinetobacter baumannii	31	57.0	1.30	62	3.4	20.3	1.1	3.7	19.6	3.3	47.53
n4	Male	49	Acinetobacter baumannii	30	66.3	6.70	85	5.8	16.7	1.4	5.9	20.1	4.2	58.19
n5	Male	44	Haemophilus	27	65.8	5.90	33	10.3	15.5	1.5	6.6	17.8	3.8	59.22
n6	Male	53	Klebsiella pneumoniae	25	111.7	4.80	95	15.2	14.8	1.8	4.3	16.8	5.1	48.64
n7	Female	51	Acinetobacter baumannii	33	124.5	3.30	121	12.1	16.9	1.2	3.8	19.5	4.4	46.90
n8	Female	57	Streptococcus pneumoniae	36	103.5	0.86	88	6.2	22.1	1.2	4.2	20.5	3.5	52.63
n9	Female	52	Streptococcus equi subsp. zooepidemicus	27	69.7	3.27	63	5.1	25.3	1.6	5.2	19.4	2.2	50.71
n10	Female	54	Enterobacter aerogenes	29	58.7	1.85	58	3.4	18.4	1.5	3.7	19.5	6.4	39.44
n11	Female	49	Candida albicans	26	76.5	1.21	61	2.9	17.1	1.3	4.8	17.9	3.1	37.89
n12	Female	37	Staphylococcus aureus	25	63.4	3.44	44	8.5	13.5	1.2	5.1	16.7	2.7	46.51

Table S2. The predicted binding free energy components for the ALX/FPR2-RvDp5 and ALX/FPR2-LXA_4 complexes using the MM/PBSA method.

	RvDp5				LXA_4			
Component [a]	**ZINC35876753**	**ZINC35876755**	**ZINC35876757**	**ZINC35876759**	**ZINC03873139**	**ZINC04556658**	**ZINC04556659**	**ZINC04556660**
ΔE_{vdw}	-54.52±3.35	-49.08±2.65	-49.17±2.61	-42.85±3.50	-44.78±3.05	-39.85±2.80	-37.86±3.59	-40.46±2.65
ΔE_{ele}	-205.19±8.32	-214.55±10.87	-195.76±20.61	-195.91±7.39	-231.04±8.65	-271.79±12.12	-273.88±11.40	-214.72±13.65
ΔE_{GB}	81.45±5.50	90.52±9.27	89.97±14.47	72.25±5.58	104.02±5.57	110.13±9.86	112.51±6.88	79.99±8.72
ΔE_{surf}	-6.01±0.21	-6.23±0.19	-6.37±0.17	-5.44±0.22	-5.29±0.16	-5.76±0.19	-5.65±0.25	-5.04±0.18
ΔG_{bind}	-184.28±3.35	-179.34±5.59	-161.33±8.16	-171.95±5.09	-177.09±7.68	-207.27±5.55	-204.89±5.80	-180.24±6.09

[a] Component: ΔE_{vdW}: van der Waals energy contribution from MM; ΔE_{ele}: electrostatic energy in the gas phase as calculated by the MM force field; ΔE_{GB}: the electrostatic contribution to the solvation free energy calculated by GB; ΔE_{surf}: nonpolar contribution to the solvation free energy calculated by solvent-accessible surface area (SASA); ΔG_{bind}: final estimated binding free energy calculated from the terms mentioned above.

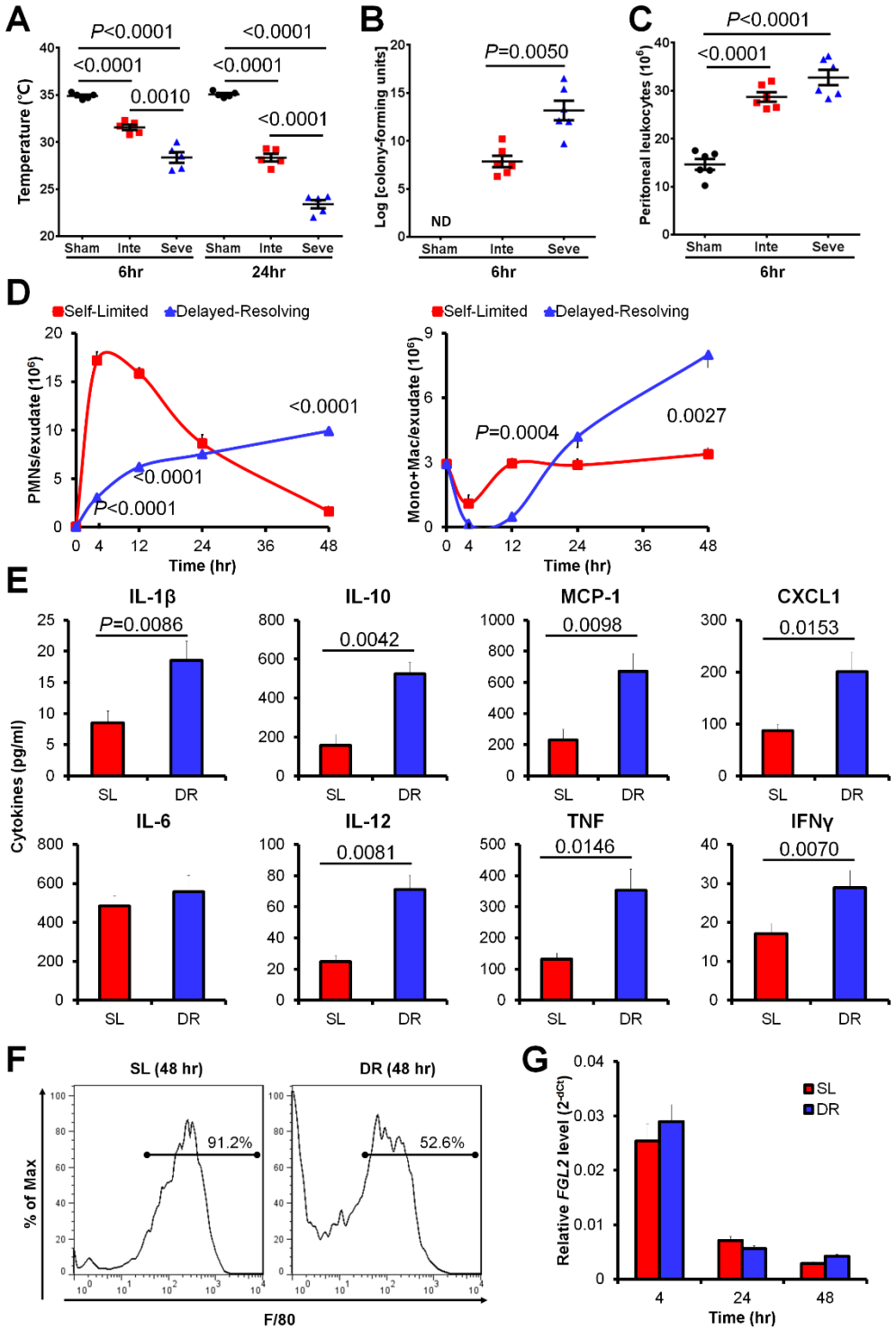

Fig. S1. Inflammation profiles in SL versus DR inflammation. (**A to C**) Mice (n=4~6) were induced different severity grades of sepsis by CLP. Temperature (**A**), aerobic bacteria levels in blood (**B**), peripheral leukocyte numbers (**C**) at indicated intervals. Inte, intermediate; Seve, severe. (**D**) PMN and mononuclear cells (monocytes and MΦs) in exudates of SL and DR peritonitis (n=3~7). (**E**) Inflammatory cytokine levels at 4 hr in SL and DR exudates (n=4). (**F**) F4/80^{+} MΦ percentages in the SL and DR exudates at 48 hr. (**G**) Fgl2 mRNA in SL and DR exudate leukocytes at 4, 24 and 48 hr (n=3~7). Error bars represent mean ± S.E.M.

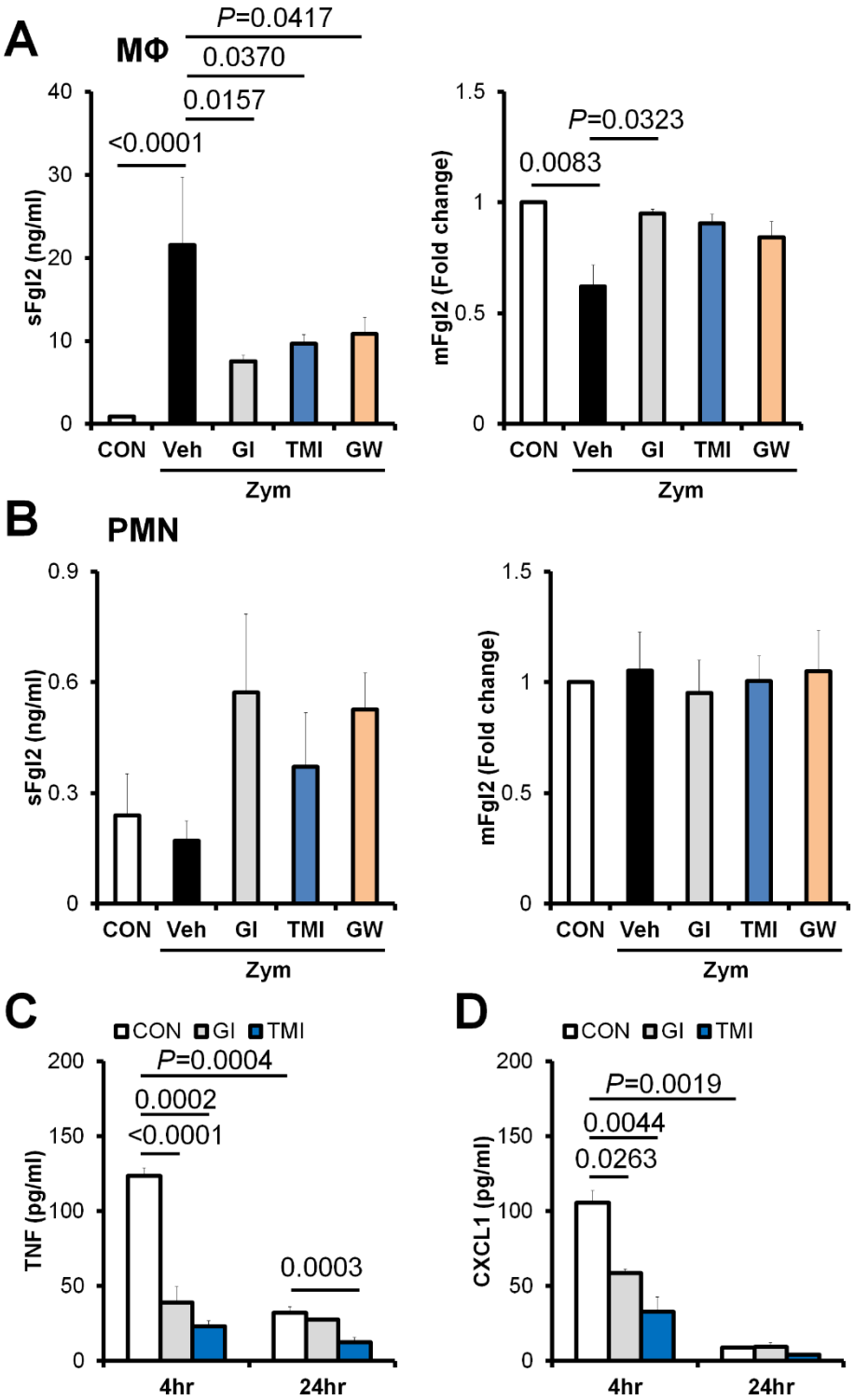

Fig. S2. Fgl2 expression is regulated by miR-466l and metalloproteinases. (**A** and **B**) Mouse bone marrow-derived MΦs (**A**) and PMNs (**B**) were treated with PBS, Zym (10 μM), with/without GI254023X, TMI-1 or GW280264X (10 μM each) for 24 hrs (MΦs) and 4 hrs (PMNs) respectively, sFgl2 and mFgl2 expression were assessed (n=3~5). (**C** and **D**) Mice were challenged *i.p.* with PBS (Veh), GI254023X (40 μg/kg), or TMI-1 (40 μg/kg), plus Zym (1 mg/mouse; n=4), the peritoneal exudate TNF (**C**) and CXCL1 (**D**) were determined with ELISA. Error bars represent mean ± S.E.M.

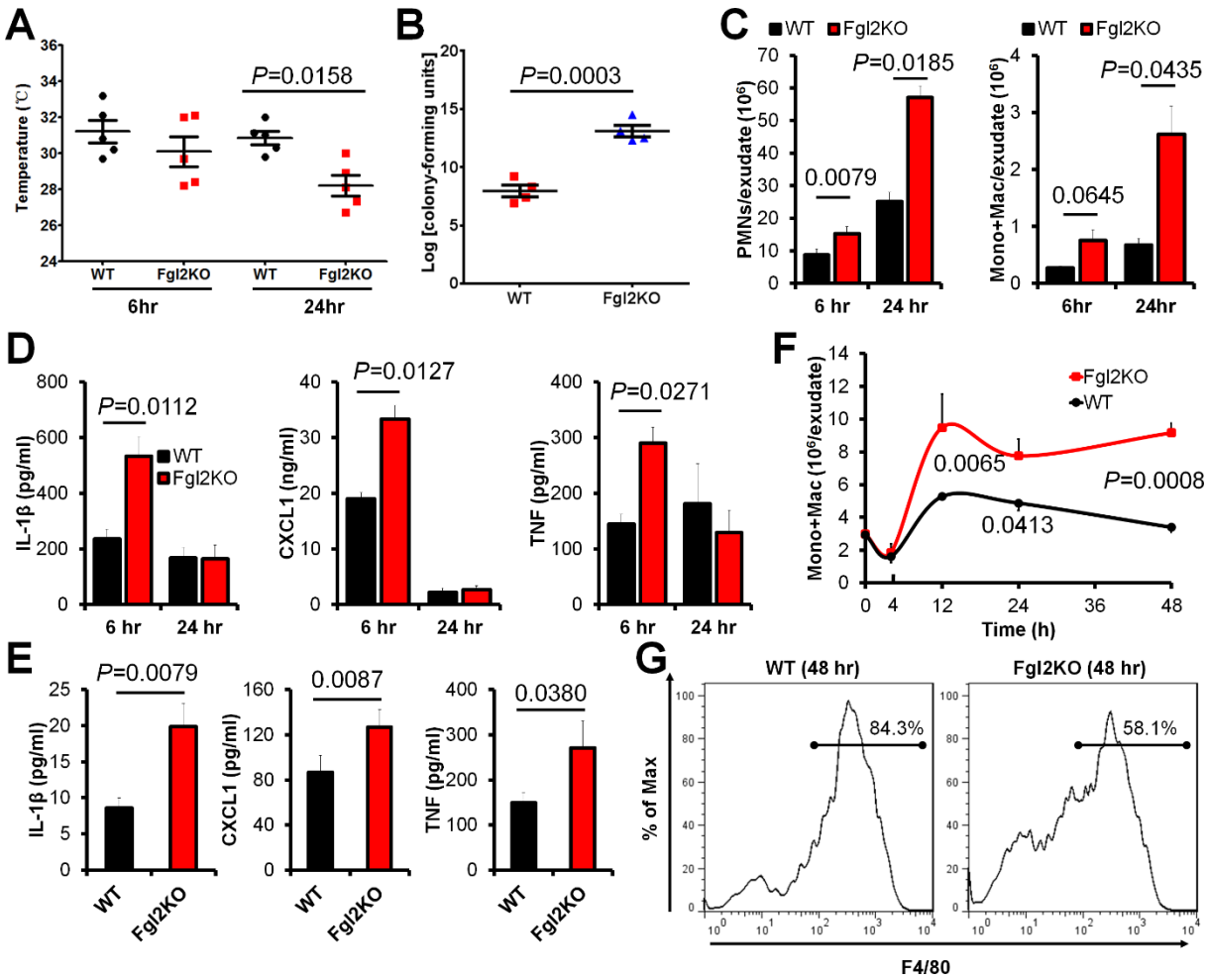

Fig. S3. Deficiency of Fgl2 promotes inflammation initiation and delays resolution. (**A to D**) Temperature (**A**), blood aerobic bacteria levels (**B**), peritoneal recruitment of PMN and mononuclear cells (**C**) and cytokine levels (**D**) in WT and Fgl2KO mice challenged with moderate CLP (n=3~5). (**E to G**) WT and Fgl2KO mice were challenged with Zym (1mg; *i.p.*). (**E**) Exudate cytokine levels (n=4). (**F**) Peritoneal mononuclear cell numbers at indicated intervals (n=4~13). (**G**) Peritoneal F4/80^{+} macrophage percentage at 48 hr (n=4). Error bars represent mean ± S.E.M.

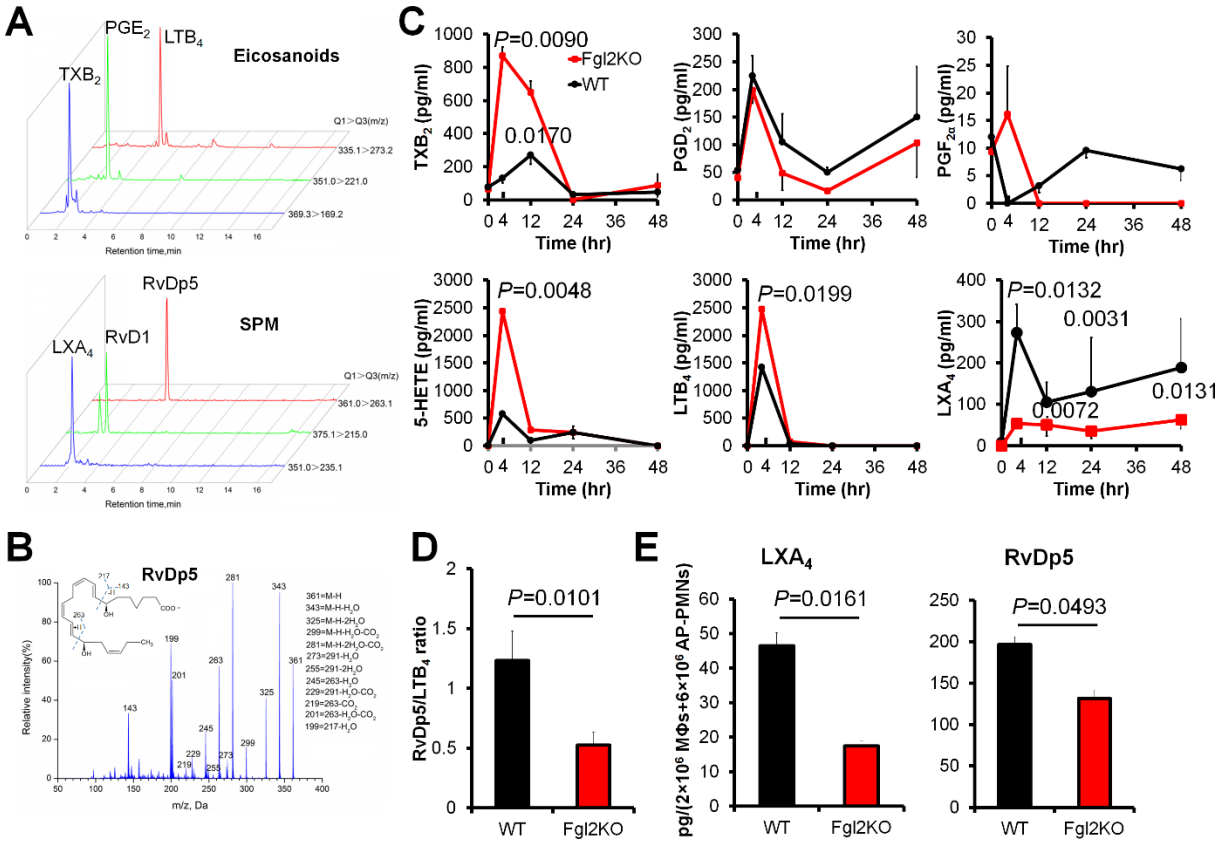

Fig. S4. Fgl2 deficiency reduces RvDp5 production. (**A to D**) WT and Fgl2KO mice were challenged with Zym (1mg; *i.p.*). Exudate LMs were identified and quantified by LC-MS-MS-based LM metabololipidomics. Representative multiple-reaction monitoring chromatograms (from three independent experiments) show the elution times for the identified bioactive LMs: Q1, M-H (parent ion); and Q3, diagnostic ion in the tandem mass spectrometry (MS/MS) (daughter ion) (**A**). MS/MS spectrum employed for the identification of RvDp5 (**B**). LM levels at indicated intervals (**C**). Ratios of SPM to pro-inflammatory LTB_4 (**D**). (**E**) Murine MΦs (2×10^6) were co-cultured with apoptotic PMNs (6×10^6) for 30 min, the cells and supernatants (n=4) were collected for determination of LXA_4 and RvDp5 with UPLC-MS/MS. Error bars represent mean ± S.E.M.

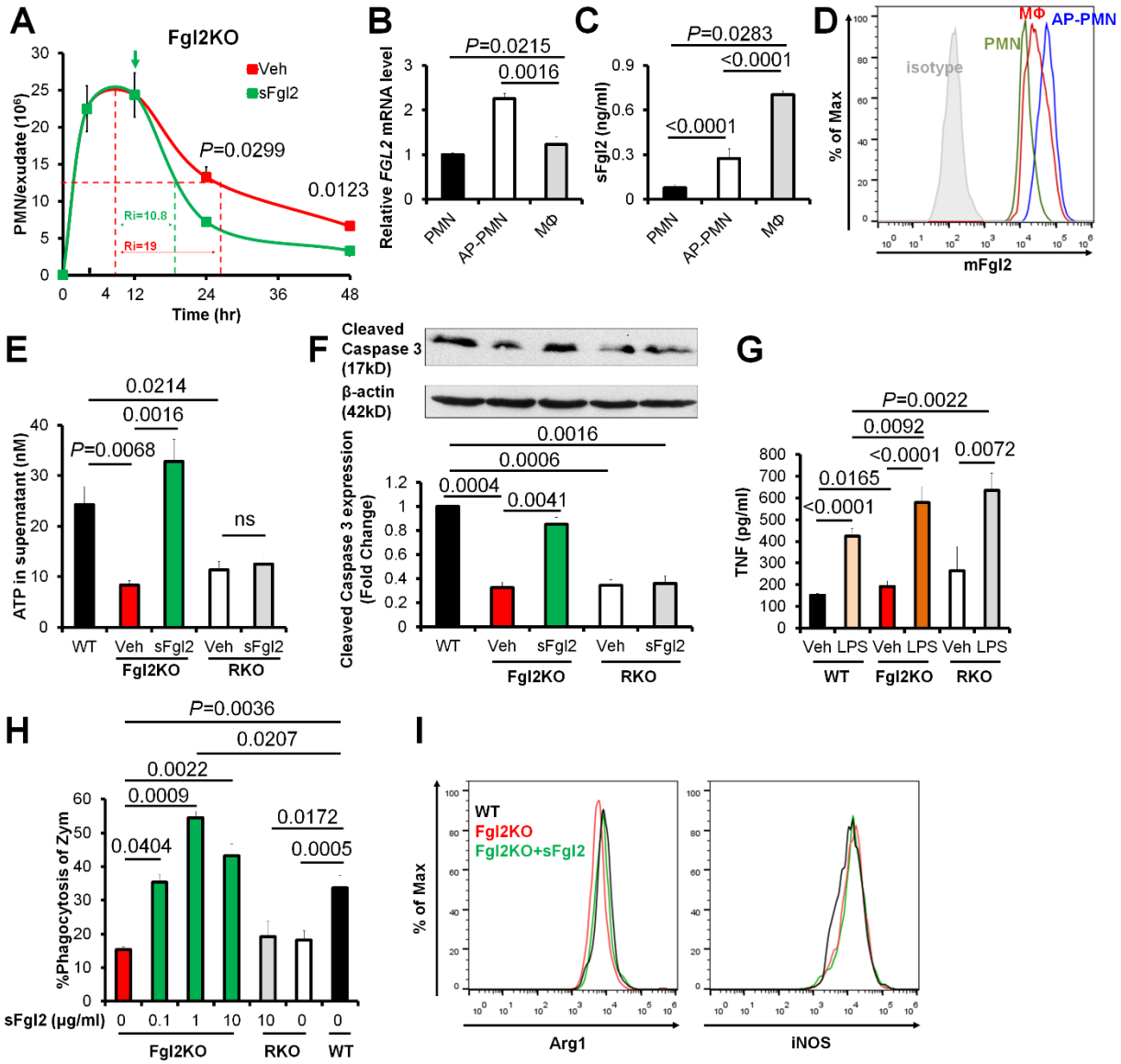

Fig. S5. Fgl2 regulates PMN apoptosis and phagocytes of MΦs. (**A**) Fgl2KO mice were injected *i.p.* with PBS (veh) or sFgl2 (200ng) at 12 hr post Zym (1 mg) intraperitoneal challenge for calculation of resolution intervals (n=3~13). (**B** to **D**) Murine BMDNs (PMNs), apoptotic PMNs (AP-PMN; PMNs cultured *in vitro* for 12 hrs) and MΦs were incubated in RPMI-1640 medium (10% FBS) for 4 hrs. The mRNA levels of *FGL2* (n=5~6) (**B**), protein expression of sFgl2 (in supernatants; n=3) (**C**) and macrophage mFgl2 (**D**) were determined with ELISA and FCM. **(E)** PMNs from WT, Fgl2KO and FcγRIIBKO (RKO) mice were induced apoptosis by UV for 2 hr with/without sFgl2 treatment (10μg/ml). ATP secretion was analyzed (n=4). (**F**) After treatment with/without sFgl2 (10 μg/ml) for 4 hrs, the expression of cleaved caspase 3 in PMNs from WT, Fgl2KO or FcγRIIB knockout (RKO) mice (n=4). (**G**) Murine peritoneal MΦs from WT, Fgl2KO and RKO mice were treated with/without LPS (1 μg/ml) for 4 hrs, the supernatant TNF were assessed with ELISA (n=3~5). (**H**) Murine peritoneal MΦs were isolated from WT, Fgl2KO (red and green) and FcγRIIBKO (RKO) mice and pretreated with/without sFgl2 for 2 hrs, and then were incubated with opsonized Zym (1:50) for 1 hr, fluorescence intensities were determined (n=4). **(I)** Murine peritoneal MΦs were isolated from WT or Fgl2KO mice, and then were treated with/without sFgl2 treatment (10 μg/ml) for 24 hrs, Arg1 and iNOS were assessed with FCM. Error bars represent mean ± S.E.M.

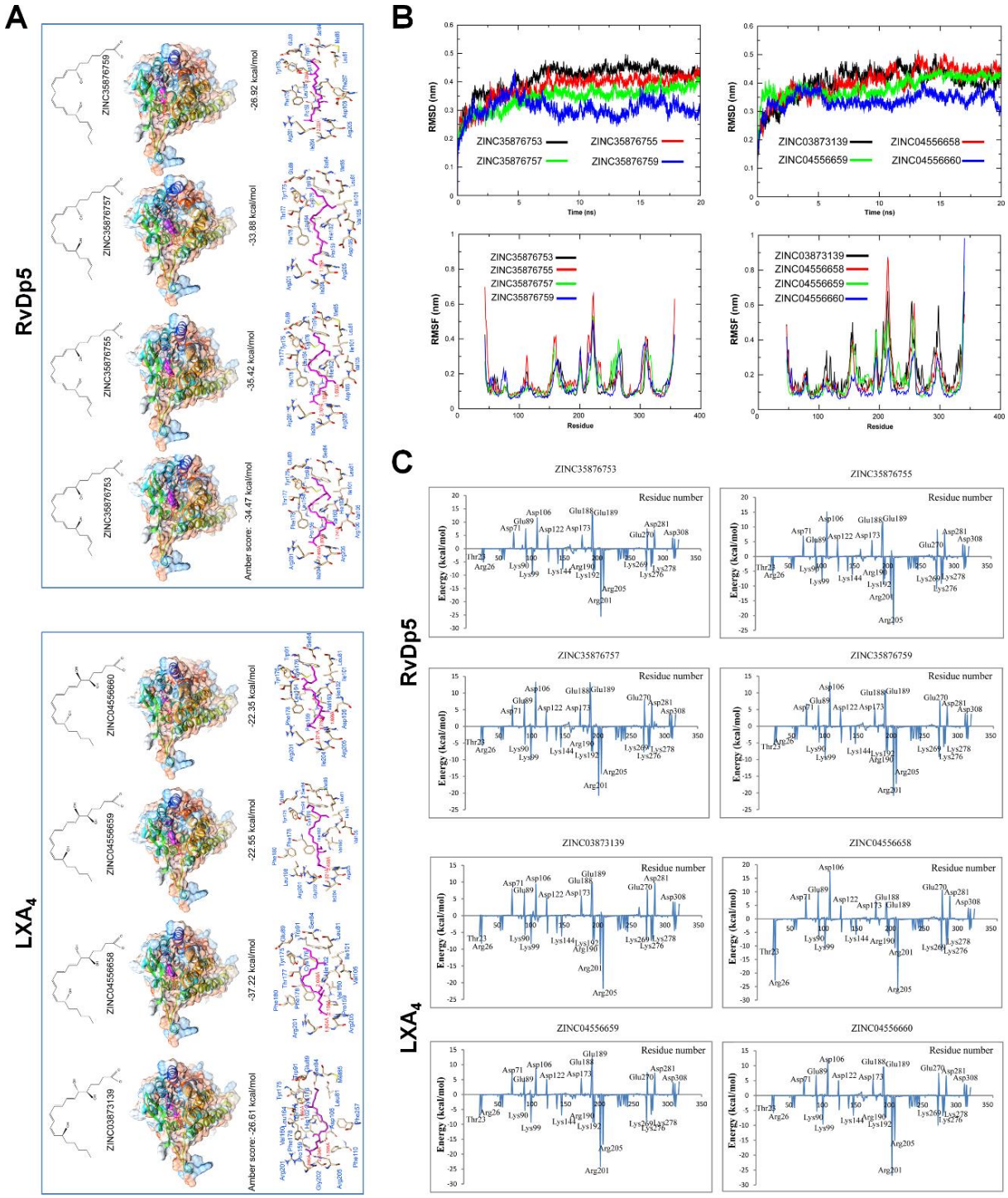

Fig. S6. An overview of binding modes for the four isomers of RvDp5 and LXA4 in the binding pocket of ALX/FPR2. (**A**) Chemical structures of RvDp5 (ZINC35876753, ZINC35876755, ZINC35876757 and ZINC35876759 were isomers) and LXA_4 (ZINC03873139, ZINC04556658, ZINC04556659 and ZINC04556660 were isomers). 3D chart of RvDp5 and LXA_4 binding with ALX/FPR2, RvDp5 was colored in magenta. Binding mode of RvDp5 (ZINC35876753, ZINC35876755, ZINC35876757 and ZINC35876759) and LXA_4 (ZINC03873139, ZINC04556658, ZINC04556659 and ZINC04556660) in the binding pocket of ALX/FPR2, important amino acid residues are shown and the red lines indicate the hydrogen bonds formed in the corresponding residues. (**B**) RMSD and RMSF of the backbone atoms of ALX/FPR2-RvDp5 and ALX/FPR2-LXA_4 complexes with respect to the initial structure during 20 ns MD simulations. (**C**) Binding free energy decomposition of ALX/FPR2-RvDp5 and ALX/FPR2-LXA_4 complexes. Statistics source data for this figure are provided in table S2.

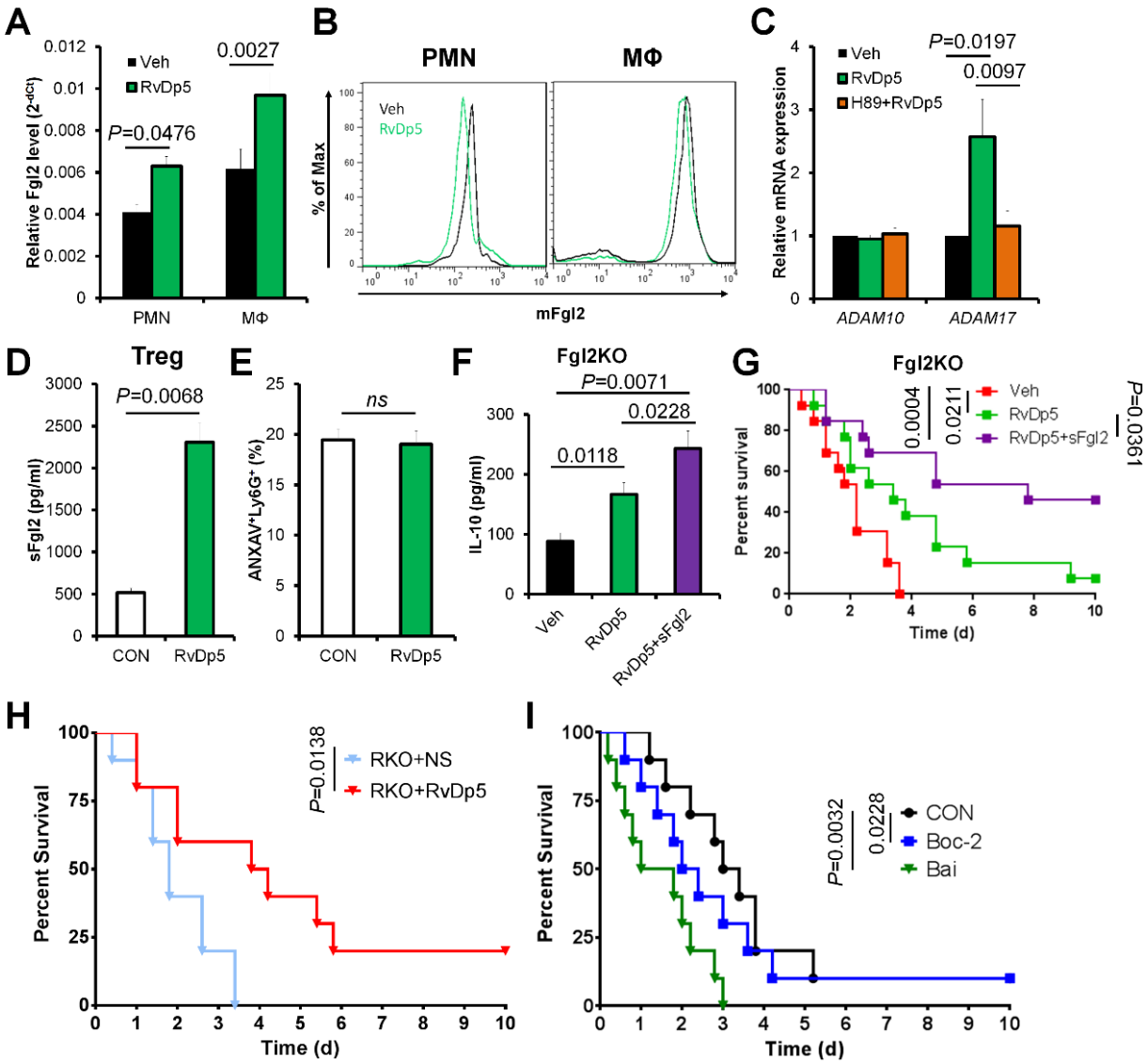

Fig. S7. RvDp5 modulates Fgl2 and improves sepsis survival. (**A and B**) Wildtype C57BL/6 mouse peripheral PMNs and peritoneal MΦs were treated with PBS (vehicle) or RvDp5 (10 nM) for 4 and 24 hrs respectively (n=4). The *FGL2* mRNA (**A**) and mFgl2 protein (**B**) were respectively assessed with qPCR and FCM. (**C**) After human MΦs were treated with PBS (Veh), RvDp5 (10 nM) with/without H89 (10 μM) for 24 hrs, the mRNA levels of ADAM10 and ADAM17 were assessed with qPCR (n=4). (**D**) Mouse spleen $CD4^+CD25^+$ Tregs were treated with PBS (Control) or RvDp5 (10 nM) for 24 hrs, the supernatant sFgl2 were determined with ELISA (n=3). (**E**) Bone marrow-derived neutrophils (n=4) were treated with or without RvDp5 (10 nM) for 4 hrs, the apoptotic PMN ($ANXAV^+Ly6G^+$) was determined with flow cytometry, ns denotes no statistical significance. (**F**) After Fgl2KO mice were injected (*i.p.*) with Zym (1mg) with or without RvDp5 (200 ng) and/or sFgl2 (200 ng) for 4 hrs, the exudate IL-10 levels were detected with ELISA. (**G**) Survival rates of Fgl2KO mice (n=13 in each group) after challenged with CLP and treated (*i.v.*) with sFgl2 (400 ng) and/or RvDp5 (300 ng). Mantel-Cox test was applied for the *P* values. (**H**) Survival rates of CLP RKO mice (n=10 each group) after treatment with NS (0.9% Natrii Chloride) or RvDp5 (300 ng). Mantel-Cox test was applied for the *P* values. (**I**) Survival rates of CLP mice (n=10) after treatment with PBS, Boc-2 (N-t-Boc-Phe-Leu-Phe-Leu-Phe, GenScript USA Inc., Piscataway, NJ, USA; 10 μg/kg) or Bai (100 mg/kg) *i.v.* (n=10 in each group). Error bars represent mean ± S.E.M.